Письма в ЭЧАЯ. 2016. Т. 13, № 4(202). С. 746–758

ON THE ROLE OF ENERGY SEPARATED IN FISSION PROCESS, EXCITATION ENERGY AND REACTION CHANNELS EFFECTS IN THE ISOMERIC RATIOS OF FISSION PRODUCT ^{135}Xe IN PHOTOFISSION OF ACTINIDE ELEMENTS

Tran Duc Thiep[a,1], *Truong Thi An*[a], *Phan Viet Cuong*[a], *Nguyen The Vinh*[a], *G. V. Mishinski*[b], *V. I. Zhemenik*[b]

[a] Institute of Physics, VAST, Ba Dinh Region, Hanoi

[b] Joint Institute for Nuclear Research, Dubna

In this work, we present the isomeric ratio of fission product ^{135}Xe in the photofission of actinide elements ^{232}Th, ^{233}U, and ^{237}Np induced by end-point bremsstrahlung energies of 13.5, 23.5, and 25.0 MeV which were determined by the method of inert gaseous flow. The data were analyzed, discussed and compared with the similar data from literature to examine the role of energy separated in fission process, excitation energy and reaction channels effects.

В работе представлены изомерные отношения в ^{135}Xe-продукте фотоделения актинидов ^{232}Th, ^{233}U и ^{237}Np, инициированного гамма-квантами тормозного спектра с конечной энергией 13,5, 23,5 и 25,0 МэВ, которые были определены с помощью метода газовой струи. Полученные данные анализируются, обсуждаются и сравниваются с соответствующими литературными данными для исследования роли энергии, выделяющейся в процессе деления, энергии возбуждения и влияния каналов реакции.

PACS: 23.35. + g; 25.85.Jg

INTRODUCTION

The isomeric ratios furnish valuable information about the energy level structure of nuclei and the nuclear reaction mechanism involved [1–5]. This ratio depends on the spin of target nucleus and the intake angular momentum determined by the mass and the energy of projectile particles. By fitting the calculated isomeric ratios based on a definite theoretical model to the experimental ones, it is possible to obtain information about the spin dependence of the nuclear level density, in particular, the spin cut-off parameter $б$ and the level density parameter a. Because of this, the study on the isomeric ratio has become one of the most effective

[1] E-mail: tdthiep@iop.vast.ac.vn, Tel: + 84-4-37564317, Fax: + 84-4-37669050

directions in the study of nuclear reaction and structure. In case of nuclear fission, the study on the isomeric ratio of the fission product allows us to interpret the mechanism of energy dissipation, which leads to better understanding of the dynamics of fission process [6, 7]. This also allows us to discuss the role of different kinds of collective movement affecting the increase of angular momentum of the product just after scission [8, 9] and leads to very important conclusions about the dependence of the angular momentum on the excitation energy of the fissioning compound nuclei [10, 11], the effects of the nuclear structure and the scission-point deformation on the product angular momentum, and the correlation of the product angular momentum with the average neutron number and elemental yield [12, 13]. Up till now most investigations have been concentrated on the study of the isomeric ratio and the angular momentum of fission product in fission of actinides with thermal and fast neutrons [12, 13, 14–21]. There are very few data on the isomeric ratio of fission products from photofission in literature and, in particular, for ^{135}Xe, the data are very rare. There is only one paper that concerns the isomeric ratio of fission products, such as ^{134}I, ^{135}Xe, ^{130}Sb, and ^{132}Sb, in the photofission of ^{237}Np and ^{238}U [22]. Therefore, the data of the isomeric ratio of ^{135}Xe in the photofission of ^{232}Th, ^{233}U, and ^{237}Np are still of great importance. In this work, we present the isomeric ratio of ^{135}Xe in photofission of ^{232}Th, ^{233}U, and ^{237}Np induced by 13.5, 23.5, and 25.0 MeV bremsstrahlungs, using the method of inert gaseous flow presented in [23, 33]. The data were analyzed, discussed and compared with the similar data from literature to examine the role of energy separated in fission process, excitation energy and reaction channels effects.

1. EXPERIMENTAL

The fission product ^{135}Xe belongs to the isobaric chain with mass number $A = 135$. During fission process, this product is directly produced from the fissioning systems ^{232}Th*, ^{233}U*, and ^{237}Np*, as well as from the beta decay of ^{135}I. Figure 1 depicts the scheme of the isobaric products ^{135}I, ^{135m,g}Xe, and ^{135}Cs for mass chain $A = 135$. The decay characteristics of ^{135m}Xe and ^{135g}Xe, which were taken from [24, 25], are presented in Table 1.

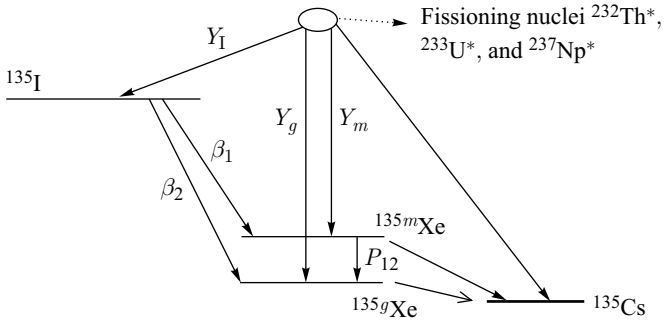

Fig. 1. Scheme of the isobaric products ^{135}I, ^{135m,g}Xe, and ^{135}Cs: Y_{I} — the cumulative yield of $^{135}_{53}$I; Y_m, Y_g — the independent yields of $^{135m}_{54}$Xe and $^{135g}_{54}$Xe, respectively; P_{12} — the coefficient of isomeric transition between $^{135m}_{54}$Xe and $^{135g}_{54}$Xe; β_1 and β_2 — the beta-decay coefficients of $^{135}_{53}$I to $^{135m}_{54}$Xe and $^{135g}_{54}$Xe, respectively

Table 1. **The decay characteristics of ^{135g}Xe and ^{135m}Xe**

^{135g}Xe ($T_{1/2}$ = 9.104 h)			^{135m}Xe ($T_{1/2}$ = 15.65 min)		
Spin, $\hbar$	Energy, keV	Intensity, %	Spin, $\hbar$	Energy, keV	Intensity, %
$3/2^+$	158.2	0.23	$11/2^-$	526.6	81.20
	358.3	0.20			
	407.9	0.32			
	608.1	2.58			
	249.7	90.60			

It is well known that the full gamma-ray spectrum from fission products is very complicated. It consists of hundreds of gamma rays and there are also gamma rays that overlap each other. Simultaneously, in this case, the dead time of measuring system and the Compton background are very high due to the high intensity of gamma rays irradiated from the fission products. This makes the identification and processing of gamma rays of interest very difficult, less accurate, or even impossible for separate ones. Therefore, in order to effectively reduce the mentioned background, various techniques, such as catcher foil technique [26, 27], fission fragment transportation [28], and chemical isotope separation [11, 18], were applied. In our case, we are interested in ^{135}Xe, which is in gaseous state. Hence, in order to determine the isomeric ratio, we used the inert gaseous flow method described in [23, 33] to transport Xe isotopes from the reaction camera to the product collector. The advantages of this method are: less time-consuming; without application of chemical isotope separation; and with simplicity in experiment and accurateness in processing of the gamma rays of interest. The experimental setup consisted of a reaction camera, product collectors, and an inert gaseous flow generator (see Fig. 2). More detailed description and operating principle of the experimental setup are shown in [23, 33]. The product collection was performed by putting the inert gas to enter the camera during and after the time of the target irradiation. Under this pressure, the inert gaseous flow will carry Xe and Kr isotopes from the reaction camera to the collectors, while all other products are caught in the reaction camera or remained on the filter. There are two collectors. The first one works during the irradiation time and collects ^{135m,g}Xe product, which is produced directly from the fissioning target and from the beta decay of ^{135}I. The second one works when the irradiation stops and collects only ^{135m,g}Xe product produced from the beta decay of ^{135}I. The gaseous products Xe and Kr were frozen in the collectors, and then the collectors were well closed and measured by semiconductor detector.

The investigated targets were thin layers of ^{232}Th, ^{233}U, and ^{237}Np with 0.1–3 mg $\cdot$ cm^{-2} thickness that were prepared on aluminum foil of 0.1 mm thickness and placed at two bottoms of the reaction camera. The target irradiation was performed by end-point bremsstrahlung produced from the electron accelerator Microtron MT-25 of the Flerov Laboratory of Nuclear Reactions, JINR, Dubna. The average electron beam was 14 μA. The description of this accelerator and its characteristics are presented in [29]. The essential advantage of this Microtron is the small energy spread of the accelerated electrons (30–40 keV) at high beam intensity (up to an average power of 600 W). This allows the measurement of the isomeric ratio at strictly definite end-point bremsstrahlung energy.

The gamma-ray spectra of the fission products in the first and second collectors were measured by a spectroscopic system consisted of an HPGe semiconductor detector (energy resolution of 1.8 keV at 1332-keV gamma ray of ^{60}Co) connected to a PC-based multichannel

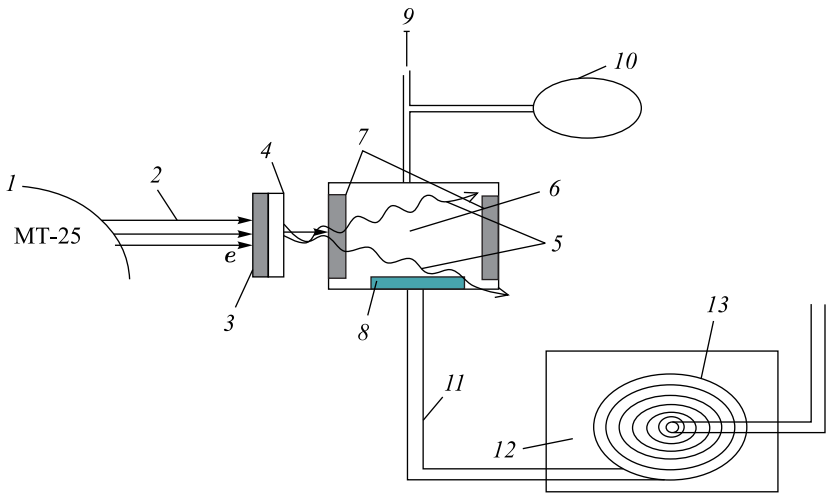

Fig. 2. The experimental setup. *1* — electron accelerator MT-25; *2* — accelerated electron beam; *3* — W-convertor of electron to photon; *4* — Al-absorber of low-energy electrons; *5* — bremsstrahlung photon flux; *6* — reaction camera; *7* — fissioning target; *8* — product filter; *9* — flow from the inert gaseous generator; *10* — manometer; *11* — capillary; *12* — cryostat; *13* — product collector

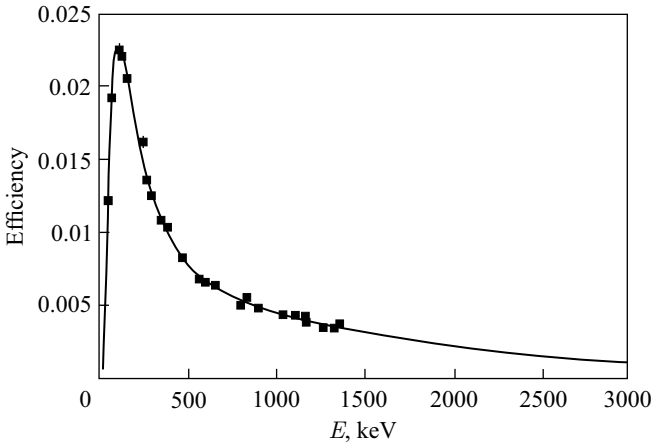

Fig. 3. The efficiency of the HPGe semiconductor detector measured at a distance of 5 cm

analyzer CANBERRA for data processing. The efficiencies of the detector were determined with a set of standard single gamma-ray sources calibrated to 1–2%. Figure 3 shows the efficiency of the detector measured at a distance of 5 cm. The measured efficiencies present curves which consist of two parts from two sides of a maximum as seen in Fig. 1. The left part for lower energies was fitted with the function as follows:

$$\ln(\varepsilon) = \sum_{i=0}^{2} a_i (\ln E)^i, \tag{1}$$

and the right part for higher energies was fitted with the function as follows:

$$\ln(\varepsilon) = \sum_{i=0}^{4} a_i (\ln E)^i, \tag{2}$$

where ε is the detection efficiency, a_i represents the fitting parameters, and E is the energy of gamma ray.

2. CALCULATION OF THE PRODUCT ISOMERIC RATIO

Based on resolving a system of equations that describe the decay processes of the isomeric and ground states of the fragment in dependence on collecting, cooling, and measurement times, we could determine the product isomeric ratio.

2.1. For the First Collector

1. For ^{135m}Xe

a) Equation for the collecting time:

$$\begin{aligned} \frac{dN_m(t)}{dt} &= Y_m - \lambda_m N_m(t) + \beta_1 \lambda_{\mathrm{I}} N_{\mathrm{I}}(t), \\ N_{\mathrm{I}}(t) &= \frac{Y_{\mathrm{I}}}{\lambda_{\mathrm{I}}}(1 - \mathrm{e}^{-\lambda_{\mathrm{I}} t}), \quad N_m(t=0) = 0. \end{aligned} \tag{3}$$

b) Equation for the cooling time:

$$\frac{dN_m(t)}{dt} = -\lambda_m N_m(t), \quad N_m(0) = N_m(t_1^{\mathrm{I}}). \tag{4}$$

c) Equation for the measurement time:

$$\frac{dN_m(t)}{dt} = -\lambda_m N_m(t), \quad N_m(0) = N_m(t_{2m}^{\mathrm{I}}). \tag{5}$$

2. For ^{135g}Xe

a) Equation for the collecting time:

$$\begin{aligned} \frac{dN_g(t)}{dt} &= Y_g - \lambda_g N_g(t) + P_{12}\lambda_m N_m(t) + \beta_2 \lambda_{\mathrm{I}} N_{\mathrm{I}}(t), \\ N_g(t=0) &= 0, \quad N_{\mathrm{I}} = \frac{Y_{\mathrm{I}}}{\lambda_{\mathrm{I}}}\left(1 - \mathrm{e}^{-\lambda_{\mathrm{I}} t}\right). \end{aligned} \tag{6}$$

b) Equation for the cooling time:

$$\frac{dN_g(t)}{dt} = -\lambda_g N_g(t) + P_{12}\lambda_m N_m(t), \quad N_g(t=0) = N_g\left(t_1^{\mathrm{I}}\right). \tag{7}$$

c) Equation for the measurement time:

$$\frac{dN_g(t)}{dt} = -\lambda_g N_g(t) + P_{12}\lambda_m N_m(t), \quad N_g(t=0) = N_g(t_{2g}^{\mathrm{I}}). \tag{8}$$

2.2. For the Second Collector

For ^{135m}Xe

a) Equation for the collecting time:

$$\begin{aligned} \frac{dN_m(t)}{dt} &= -\lambda_m N_m(t) + \beta_1 \lambda_{\mathrm{I}} N_{\mathrm{I}}(t), \\ N_{\mathrm{I}}(t) &= \frac{Y_{\mathrm{I}}}{\lambda_{\mathrm{I}}}(1 - \mathrm{e}^{-\lambda_{\mathrm{I}}})\,\mathrm{e}^{-\lambda_{\mathrm{I}} t_c}\,\mathrm{e}^{-\lambda_{\mathrm{I}} t}, \quad N_m(t=0) = 0. \end{aligned} \tag{9}$$

b) Equation for the cooling time:

$$\frac{dN_m(t)}{dt} = -\lambda_m N_m(t), \quad N_m(t=0) = N_m(t_1^{\mathrm{II}}). \tag{10}$$

c) Equation for the measurement time:

$$\frac{dN_m(t)}{dt} = -\lambda_m N_m(t), \quad N_m(t=0) = N_m(t_{2m}^{\mathrm{I}}). \tag{11}$$

By resolving the above equation system and taking into account that in practice the numbers of gamma rays are measured instead of the numbers of radioactive nuclei, we obtained the following expressions:

$$\frac{S_m^{\mathrm{I}}}{\varepsilon_m^{\mathrm{I}} I_m} = Y_m \Lambda_1 \Lambda_2 \Lambda_3 + Y_{\mathrm{I}} \Lambda_4 \Lambda_2 \Lambda_3, \tag{12}$$

$$\begin{aligned} \frac{S_g^{\mathrm{I}}}{\varepsilon_g^{\mathrm{I}} I_g} = {} & Y_g \Lambda_5 \Lambda_9^g \Lambda_{11} + Y_m(\Lambda_6 \Lambda_9^g \Lambda_{11} + \Lambda_1 \Lambda_{10} \Lambda_{11} + \Lambda_1 \Lambda_9^m \Lambda_{12}) + \\ & + Y_{\mathrm{I}}(\Lambda_7 \Lambda_9^g \Lambda_{11} + \Lambda_8 \Lambda_9^g \Lambda_{11} + \Lambda_4 \Lambda_{10} \Lambda_{11} + \Lambda_9^m \Lambda_4 \Lambda_{11}), \end{aligned} \tag{13}$$

$$\frac{S_m^{\mathrm{II}}}{\varepsilon_m^{\mathrm{II}} I_m} = Y_{\mathrm{I}} \Lambda_{13} \Lambda_{14} \Lambda_{15} \Lambda_{16} \Lambda_{17}. \tag{14}$$

We obtained from formulas (12), (13), and (14) the following expressions for the independent yields of ^{135m}Xe and ^{135g}Xe:

$$Y_m = \frac{\dfrac{S_m^{\mathrm{I}}}{\varepsilon_m^{\mathrm{I}} I_m} - \dfrac{S_m^{\mathrm{II}}}{\varepsilon_m^{\mathrm{II}} I_m} \dfrac{\Lambda_4 \Lambda_2 \Lambda_3}{\Lambda_{13} \Lambda_{14} \Lambda_{15} \Lambda_{16} \Lambda_{17}}}{\Lambda_1 \Lambda_2 \Lambda_3}, \tag{15}$$

$$\begin{aligned} Y_g = {} & \frac{\Lambda_1 \Lambda_2 \Lambda_3 \left(\dfrac{S_g^{\mathrm{I}}}{\varepsilon_g^{\mathrm{I}} I_g} - \dfrac{S_m^{\mathrm{II}}}{\varepsilon_m^{\mathrm{II}} I_m} \dfrac{(\Lambda_7 \Lambda_9^g \Lambda_{11} + \Lambda_8 \Lambda_9^g \Lambda_{11} + \Lambda_4 \Lambda_{10} \Lambda_{11} + \Lambda_9^g \Lambda_4 \Lambda_{12})}{\Lambda_{13} \Lambda_{14} \Lambda_{15} \Lambda_{16} \Lambda_{17}} \right)}{\Lambda_1 \Lambda_2 \Lambda_3 \Lambda_5 \Lambda_9^g \Lambda_{11}} - \\ & - \frac{(\Lambda_6 \Lambda_9^g \Lambda_{11} + \Lambda_1 \Lambda_{10} \Lambda_{11} + \Lambda_1 \Lambda_9^g \Lambda_{12}) \left(\dfrac{S_m^{\mathrm{I}}}{\varepsilon_m^{\mathrm{I}} I_m} - \dfrac{S_m^{\mathrm{II}}}{\varepsilon_m^{\mathrm{II}} I_m} \dfrac{\Lambda_4 \Lambda_2 \Lambda_3}{\Lambda_{13} \Lambda_{14} \Lambda_{15} \Lambda_{16} \Lambda_{17}} \right)}{\Lambda_1 \Lambda_2 \Lambda_3 \Lambda_5 \Lambda_9^g \Lambda_{11}}. \end{aligned} \tag{16}$$

The isomeric ratio of fission product is defined as

$$\mathrm{IR} = \frac{Y_m}{Y_g}, \tag{17}$$

where Λ_i ($i = 1$–17) are the expressions connected to the collecting, cooling, and measurement times in the first and second collectors; S — the counts under gamma rays characterizing the isomeric and ground states; I and II — the first and second collectors; I_m and I_g — the intensities of the isomeric and ground states; Y — the product yield; ε — the detection efficiency; m and g — the isomeric and ground states; N_m, N_g, and λ_m, λ_g — the numbers of $^{135m}_{54}$Xe and $^{135g}_{54}$Xe and their decay constants, respectively; N_{I}, λ_{I} — the number of ^{135}I and its decay constant; and P_{12} — the coefficient of isomeric transition between $^{135m}_{54}$Xe and $^{135g}_{54}$Xe.

3. RESULTS AND DISCUSSION

Figure 4 shows a typical gamma-ray spectrum of the photofission of ^{232}Th by using catcher foil technique [26, 27]. One can see that the spectrum is very complicated. In this work, with the use of the method of the inert gaseous flow, all products were caught in the reaction camera or remained on the filter, except gaseous products Xe and Kr. Therefore, the

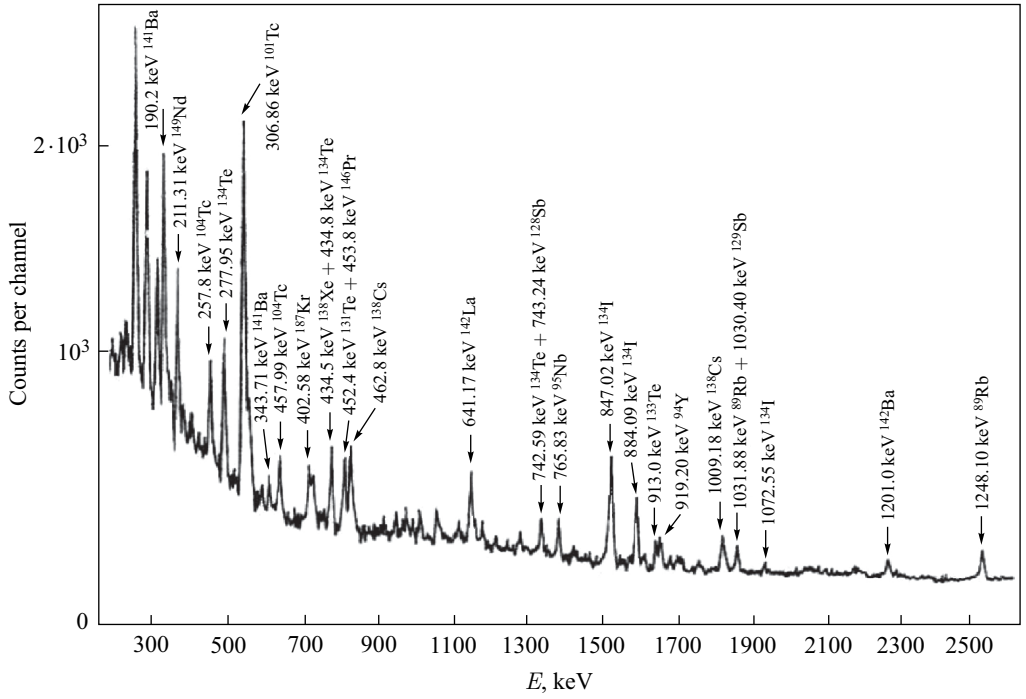

Fig. 4. A typical gamma-ray spectrum of the photofission of ^{232}Th measured by using catcher foil technique for times of irradiation, cooling, and measurement of 240, 30, and 10 min, respectively

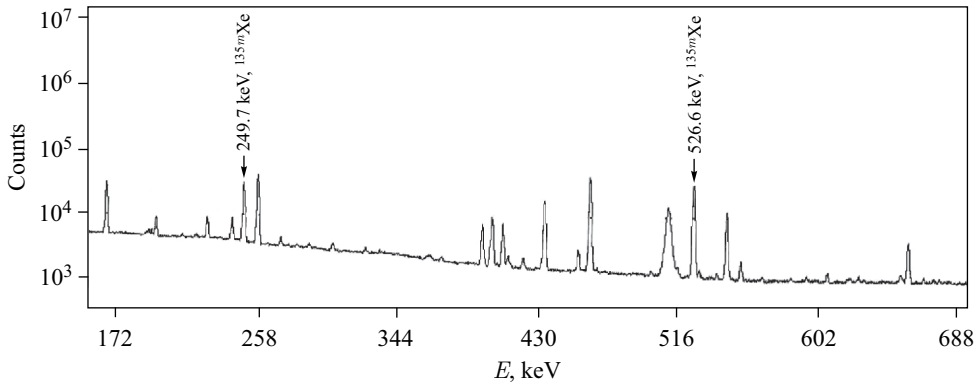

Fig. 5. A part of the gamma-ray spectrum of the photofission of ^{237}Np induced by end-point bremsstrahlung energy of 25.0 MeV measured for the first collector

gamma-ray spectrum was very simple due to the fact that the background from other products was eliminated. As a demonstration of the experimental procedure in Fig. 5 a part of the gamma-ray spectrum is shown measured for the first collector in the case of the photofission of ^{237}Np induced by end-point bremsstrahlung energy of 25.0 MeV. The characteristic gamma rays of the isomeric and ground states of ^{135}Xe are seen very clearly. One can see that in this case, the gamma-ray spectrum is very simple in comparison with the gamma spectrum shown in Fig. 4. This made the identification and processing of gamma rays of interest very simple and more accurate. The isomeric ratio was determined by the method shown in [23, 33] as the average value $\overline{\text{IR}}$ of those data calculated from various combinations of a series of gamma-ray spectra measured for the first and second collectors with different times of cooling and measurement. Two gamma rays of 249.7 and 526.6 keV were used for determination of the isomeric ratio due to their high intensities.

The relative error was determined by the following formula:

$$\varepsilon(\overline{\text{IR}}) = \frac{\sigma(\overline{\text{IR}})}{\overline{\text{IR}}} = \frac{\sqrt{\sum_{i=1}^{n}\sigma_i^2(\text{IR})\Big/ n}}{\overline{\text{IR}}}, \tag{18}$$

where σ_i (IR) is the error of the isomeric ratio calculated for i, the combination of measurements, and n is the number of combinations of the measurement.

Table 2 shows the results of our experiment for the isomeric ratio of ^{135}Xe in the photofission of ^{232}Th, ^{233}U, and ^{237}Np induced by end-point bremsstrahlung energies of 13.5, 23.5, and 25.0 MeV. As the data for the isomeric ratio of ^{135}Xe in the photofission of ^{232}Th* and ^{233}U* are not available in the literature we were unable to make any comparison with our results. Table 2 also shows the isomeric ratios in product ^{135}Xe in the case of fission of ^{232}U and ^{233}U induced by thermal neutron [12, 14–16] and of ^{232}Th induced by fast neutron [12]. In order to clarify the experimental result, we also show the isomeric ratio of ^{135}Xe obtained in our work and that from [22] for the photofission of ^{237}Np. It is worth noting that authors in [22] used a conventional gamma spectroscopic method, while we used the inert gaseous flow one. Here one can see that our result for ^{237}Np is in agreement with

Table 2. **The isomeric ratio of ^{135}Xe in fission with neutron and bremsstrahlung**

Target	Nuclear reaction	Fissioning nuclei	Product	Neutron projectile	Bremsstrahlung projectile
^{232}Th	^{232}Th(n,f) ^{233}Th	^{233}Th*	^{135}Xe	1.301 ± 0.230 [12] (fast neutron)	
^{232}Th	^{232}Th(γ,f) ^{232}Th	^{232}Th*	^{135}Xe		0.837 ± 0.095 [23], our work (13.5-MeV bremsstrahlung) 1.346 ± 0.094 (this work) (23.5-MeV bremsstrahlung) 1.397 ± 0.097 (this work) (25.0-MeV bremsstrahlung)
^{233}U	^{233}U(n,f) ^{234}U	^{234}U*	^{135}Xe	1.241 ± 0.201 [14] 1.602 ± 0.112 [15] 1.271 ± 0.110 [15] 1.642 ± 0.160 [12] 1.471 ± 0.141 [16] (thermal neutron)	
^{232}U	^{232}U(n,f) ^{233}U	^{233}U*	^{135}Xe		
^{233}U	^{233}U(γ,f) ^{233}U	^{233}U*	^{135}Xe		0.906 ± 0.121 [23], our work (13.5-MeV bremsstrahlung) 1.694 ± 0.248 [33], our work (23.5-MeV bremsstrahlung) 1.726 ± 0.253 (this work) (25.0-MeV bremsstrahlung)
^{237}Np	^{237}Np(γ,f) ^{237}Np	^{237}Np*	^{135}Xe		0.610 ± 0.060 [22] (16-MeV bremsstrahlung) 0.863 ± 0.103 [23], our work (13.5-MeV bremsstrahlung) 1.386 ± 0.1622 (this work) (23.5-MeV bremsstrahlung) 1.410 ± 0.180 (this work) (25.0-MeV bremsstrahlung)
^{134}Xe	^{134}Xe(n,γ) ^{135}Xe		^{135}Xe	0.013 [30] (thermal neutron)	
^{136}Xe	^{136}Xe(γ,n) ^{135}Xe		^{135}Xe		0.11 [30] (23.5-MeV bremsstrahlung)
^{136}Xe	^{136}Xe$(n,2n)$ ^{135}Xe		^{135}Xe	0.49 ± 0.04 [34] (14.5-MeV neutron)	

that from [22]. It can also be seen from Table 2 that in the photofission of ^{233}U induced by end-point bremsstrahlung energies of 23.5 and 25.0 MeV, the isomeric ratios of ^{135}Xe are in the same order with that by thermal neutron fission of ^{232}U and ^{233}U. For the case of the photofission of ^{232}Th, the isomeric ratio of ^{135}Xe is in the same order with that in fission of ^{232}Th induced by fast neutron.

From the obtained results, one can see the facts that, in general, the isomeric cross-section ratio is expected to depend on several factors, such as spin of the target nuclei, type of projectile and its energy used, type of emitted particles, type of nuclear reactions and, more

important, on the spin of the isomeric states concerned. Our results led to the following effects:

3.1. The Role of the Excitation Energy and Impulse. One can see from Table 2 that for photofissions of ^{232}Th, ^{233}U, and ^{237}Np, the isomeric ratio of product ^{135}Xe increases with the increase of end-point energy bremsstrahlungs. This means that the higher is the projectile energy (or impulse), the higher is the isomeric ratio; i.e., the probability of forming the high-spin state increases faster than that for the low-spin one, when the end-point energy bremsstrahlung (or impulse) increases. This fact shows the role of the excitation energy and impulse.

3.2. The Effect of Reaction Channels. In our case, the reaction product ^{135m,g}Xe is produced from four reactions, namely, from three one-step reactions $^{134}\mathrm{Xe}(n,\gamma)\,^{135m,g}\mathrm{Xe}$, $^{136}\mathrm{Xe}(\gamma,n)\,^{135m,g}\mathrm{Xe}$, $^{136}\mathrm{Xe}(n,2n)\,^{135m,g}\mathrm{Xe}$, and the photofission of ^{232}Th, ^{233}U, and ^{237}Np, i.e., from (n,γ), (γ,n), $(n,2n)$, and (γ,f) reaction channels. As is seen from Table 2, the isomeric ratios of isomeric pair ^{135m,g}Xe in the above-mentioned reactions are 0.013 [30]; 0.11 [30]; 0.49 $\pm$ 0.04 [34] and 0.906 $\pm$ 0.121; 0.837 $\pm$ 0.095; 0.863 $\pm$ 0.103 (for the case of 13.5-MeV bremsstrahlung), respectively. It can be said that the difference in the isomeric ratios in the above-mentioned reactions is due to the influence of the effect of reaction channels. The difference of the isomeric ratio is very big between one-step reactions and the fission ones. From Table 2 the channel effect from photofission and fission induced by fast and thermal neutrons on the isomeric ratio of ^{135m,g}Xe product can also be seen. However, in this case, the difference of the isomeric ratio is very small and it may be due to the small difference in mechanism of fission processes induced by fast, thermal neutrons, and bremsstrahlungs. Therefore, the study of the isomeric ratio of ^{135m,g}Xe led to the conclusion that the more is the reaction mechanism difference, the bigger is the channel influence. The channel effect has also been observed in [31, 32] for other reactions which lead to the same products. In [31], the authors studied the isomeric ratio in ^{69m,g}Zn produced from $^{72}\mathrm{Ge}(n,\alpha)\,^{69m,g}\mathrm{Zn}$, $^{69}\mathrm{Ga}(n,p)\,^{69m,g}\mathrm{Zn}$, and $^{70}\mathrm{Zn}(n,2n)\,^{69m,g}\mathrm{Zn}$ reactions, as well as the isomeric ratio in ^{71m,g}Zn formed in $^{69}\mathrm{Ge}(n,\alpha)\,^{71m,g}\mathrm{Zn}$ and $^{71}\mathrm{Ga}(n,p)\,^{71m,g}\mathrm{Zn}$ and showed the effects of reaction channels on the isomeric cross-section ratios. In [32], the influence of reaction channels on the isomeric cross-section ratio was investigated by analyzing the experimental data on reactions $^{52}\mathrm{Cr}(p,n)\,^{52m,g}\mathrm{Mn}$, $^{52}\mathrm{Cr}(^3\mathrm{He},\ t)\,^{52m,g}\mathrm{Mn}$, $^{54}\mathrm{Fe}(d,\alpha)\,^{52m,g}\mathrm{Mn}$, $^{54}\mathrm{Fe}(n,t)\,^{52m,g}\mathrm{Mn}$, and $^{52}\mathrm{Cr}(^3\mathrm{He};p,\alpha)\,^{52m,g}\mathrm{Mn}$ over the incident particle energy up to 35 MeV. The investigation led to the conclusion that the influence is most pronounced when the reaction channels differ widely, i.e., (p,n) and $(^3\mathrm{He},\ t)$ processes.

3.3. The Role of Energy Separated in Fission Process. It is very interesting to note that the isomeric ratio of ^{135}Xe in the photofission of ^{232}Th, ^{233}U, and ^{237}Np is much higher than that of ^{135}Xe formed in one-step reactions $^{134}\mathrm{Xe}(n,\gamma)\,^{135m,g}\mathrm{Xe}$ (IR $=$ 0.013) [30], $^{136}\mathrm{Xe}(\gamma,n)\,^{135m,g}\mathrm{Xe}$ (IR $=$ 0.11) [30], and $^{136}\mathrm{Xe}(n,2n)\,^{135m,g}\mathrm{Xe}$ (IR $=$ 0.49 $\pm$ 0.04) [34]. This may lead to additional mechanism of increasing the isomeric ratio and the angular momentum of fission fragments just after scission. Let us consider the case of 23.5-MeV bremsstrahlung. Although the photofission was induced by the end-point bremsstrahlung energy of 23.5 MeV, the main contribution carrying in the giant resonance region is about 15.0 MeV, i.e., equivalent to the excitation energy in $^{136}\mathrm{Xe}(n,2n)\,^{135m,g}\mathrm{Xe}$ reaction (IR $=$ 0.49 $\pm$ 0.04) [34]. This energy and a part of the energy separated in the fission process led to higher excitation energy of fission fragments and emission of neutron from them. As a result, the isomeric ratio of product in the fission process is higher than that in

the one-step (n,γ), (γ,n), and $(n,2n)$ reactions. The energy separated in the fission process can be seen clearly from the following formulas:

$$E^*_{\rm CN} = \frac{\int\limits_{B_f}^{E_e} E\sigma(\gamma,t)\,\phi(E_e,E)\,dE}{\int\limits_{B_f}^{E_e} \sigma(\gamma,f)\,\phi(E_e,E)\,dE}, \tag{19}$$

$$E^*_f = E^*_{\rm CN} + Q - {\rm TKE}'. \tag{20}$$

In formulas (19) and (20), B_f — the fission barrier; $\sigma(\gamma,f)$ — the photofission cross section; $\phi(E_e,E)$ — the bremsstrahlung spectrum; E_e — the electron energy or end-point bremsstrahlung energy; Q — the mass defect difference before and after reaction; TKE′ — the total kinetic energy of fission fragments; $E^*_{\rm CN}$ — the mean excitation energy of compound nuclei; and E^*_f — the total excitation energy of fragments. Furthermore, it was assumed that the total excitation energy of fragments is proportionally divided between their atomic masses. From formula (20) one can see that a part of the energy, namely, Q–TKE′ separated in the fission process leads to higher excitation energy of product and higher isomeric ratio. On the other hand, as fission is a complicated nuclear process, the high value of the isomeric ratio of fission product in comparison with other reaction is expected to come from the mechanism of energy dissipation, different kinds of collective movement affecting the increase of angular momentum of the product just after scission, and so on.

It is worth noting that fission product ^{135}Xe was selected to investigate the isomeric ratio due to the fact that ^{135}Xe can be formed not only from the fission, but also in $^{134}{\rm Xe}(n,\gamma)\,^{135m,g}{\rm Xe}$, $^{136}{\rm Xe}(\gamma,n)\,^{135m,g}{\rm Xe}$, and $^{136}{\rm Xe}(n,2n)\,^{135m,g}{\rm Xe}$ one-step reactions. The mechanism of these one-step reactions is well known and the angular momenta of absorbed γ quantum and the energy of emitted neutron are fixed. Therefore, in the case of these reactions, it was possible to perform a detailed calculation of change in the angular momentum of nucleus ^{135}Xe at population of the isomeric and ground states, and then from the isomeric ratio of nucleus ^{135}Xe the parameters of level density, which could be used for the model calculation of the angular momentum of photofission product ^{135}Xe, can be obtained.

CONCLUSIONS

In this work, we have presented the data for the isomeric ratio of ^{135}Xe product in the photofission of ^{232}Th, ^{233}U, and ^{237}Np induced by 13.5-, 23.5-, and 25.0-MeV bremsstrahlungs using the method of inert gaseous flow. The obtained data show the following facts: a) the isomeric ratio of fission product increases with the increase of bremsstrahlung energy (i.e., excitation energy); b) the isomeric ratio of ^{135}Xe in the photofission of ^{232}Th, ^{233}U, and ^{237}Np is much higher than that of ^{135}Xe formed in $^{134}{\rm Xe}(n,\gamma)\,^{135m,g}{\rm Xe}$, $^{136}{\rm Xe}(\gamma,n)\,^{135m,g}{\rm Xe}$, and $^{136}{\rm Xe}(n,2n)\,^{135m,g}{\rm Xe}$ one-step reactions; and c) the isomeric ratio of ^{134}Xe is different in $^{134}{\rm Xe}(n,\gamma)^{135m,g}{\rm Xe}$, $^{136}{\rm Xe}(\gamma,n)^{135m,g}{\rm Xe}$, and $^{136}{\rm Xe}(n,2n)^{135m,g}{\rm Xe}$ one-step reactions, and in photofission and fission with thermal and fast neutrons; and the more complicated is the reaction mechanism, the bigger is the isomeric ratio difference. The above-mentioned facts

demonstrate the role of excitation energy and impulse, energy separated in fission process and reaction channels effects in the isomeric ratio of fission product ^{135}Xe from the photofission of actinide elements. The obtained results in this work could contribute to the Nuclear Data.

This work has been performed at the Flerov Laboratory of Nuclear Reactions, Joint Institute for Nuclear Research, Dubna, Russia. The authors would like to recall with gratitude the name of deceased Prof. Yu. P. Gangrsky for his interest to this work and to thank A. G. Belov and his working team on Microtron MT-25 for operating the accelerator facility and G. V. Buklanov for the target preparation.

The Vietnamese authors would like to thank for the support from the Institute of Physics, Vietnam Academy of Science and Technology.

REFERENCES

1. *Huizenga J. R., Vandenbosch R.* Interpretation of Isomeric Cross-Section Ratios for (n, γ) and (γ, n) Reactions // Phys. Rev. 1960. V. 120. P. 1306.
2. *Huizenga J. R., Vandenbosch R.* Isomeric Cross-Section Ratios for Reactions Producing the Isomeric Pair ^{197,197m}Hg // Ibid. P. 1313.
3. *Kolev D., Ernest J.* The Role of Angular Momentum Removal in Photonuclear Reactions as Deduced from the Isomeric Ratios for ^{120m,g}Sb and ^{117m,g}In // Phys. G: Nucl. Part. Phys. 1998. V. 24. P. 589.
4. *Bartsch H. et al.* Critical Consideration of the Statistical Model Analysis of Photonuclear Isomeric Cross-Section Ratios // Nucl. Phys. A. 1976. V. 256. P. 243.
5. *Karamian S. A. et al.* Isomeric to Ground-State Ratio in the ^{180}Ta$^m(\gamma, \gamma')\,^{93}$Ta^{180m,g} Reaction // Phys. Rev. C. 1998. V. 57, No. 4. P. 1812.
6. *Denschlag H. O. et al.* Distributions of Nuclear Charge and Angular Momentum in Chains 132–137, 99, and 102 of ^{235}U(n_{th}, f) at Various Kinetic Energies and Ionic Charge States of the Fragments // Proc. of the Intern. Symp. on the Physics and Chemistry of Fission, Jülich, 1979. IAEA. Vienna, 1980. V. 2. P. 153.
7. *Hondt P. D. et al.* Energy Distributions and Absolute Yield of the Charge Light Particles Emitted during the Thermal Neutron-Induced Ternary Fission of ^{235}U // Nucl. Phys. A. 1980. V. 346. P. 461.
8. *Nix J. R., Swiatecki W. J.* Studies in the Liquid-Drop Theory of Nuclear Fission // Nucl. Phys. 1965. V. 71. P. 1.
9. *Rasmusse J. O., Norenberg W., Mang H. J.* A Model for Calculating the Angular Momentum Distribution of Fission Fragment // Nucl. Phys. A. 1969. V. 136. P. 465.
10. *Thierens H. et al.* Independent Isomeric Yield Ratio of ^{134}I in the Photofission of ^{235}U and ^{238}U // Phys. Rev. C. 1982. V. 25. P. 1546.
11. *Tonchev A. P. et al.* Isomeric Yield Ratio of ^{134}I in Photofission of ^{232}Th and ^{238}U // Radioanal. Nucl. Chem. 1991. V. 155, No. 5. P. 299.
12. *Naik H., Dange S. P., Singh R. J.* Angular Momentum of Fission Fragments in Low-Energy Fission of Actinides // Phys. Rev. C. 2005. V. 71. 014304.
13. *Naik H. et al.* Correlations of Fission Fragment Angular Momentum with Collective and Intrinsic Degrees of Freedom // Z. Phys. A. At. Nucl. 1988. V. 331. P. 335.
14. *Ford G. P., Wolfsberg K., Erdal B. R.* Independent Yields of Isomers of ^{133}Xe and ^{135}Xe for Neutron-Induced Fission of ^{233}U, ^{235}U, ^{238}U, ^{239}P, and ^{242m}Am // Phys. Rev. C. 1984. V. 30, No. 1. P. 195.

15. *Fujiwara I., Imanishi N., Nishi T.* Isomer-Yield Ratios and Primary Angular Momenta of I, Xe, and Cs Isotopes Produced in Thermal-Neutron Fission of ^{233}U, ^{235}U, and ^{239}Pu // Phys. Soc. Japan. 1982. V. 51. P. 1713.
16. *Haddad M. et al.* Post-Neutron Mass Distribution for $^{232}\mathrm{U}(n_{\mathrm{th}}, f)$ // Radiochem. Acta. 1989. V. 46. P. 23.
17. *Naik H. et al.* Systematics of Fragment Angular Momentum in Low-Energy Fission of Actinides // Nucl. Phys. A. 1995. V. 587. P. 273.
18. *Hsu S. S. et al.* Yields and Isomeric Ratio of Xenon and Krypton Isotopes from Thermal Neutron Fission of ^{235}U // Phys. Rev. C. 1981. V. 24, No. 2. P. 523.
19. *Aumann D. C. et al.* Independent Isomeric Yield Ratio of ^{148}Pm in Fission of the Moderately Excited ^{236}U Compound Nucleus as a Measure of Fragment Angular Momentum // Phys. Rev. C. 1977. V. 16, No. 1. P. 254.
20. *Vyshnevskyi I. N. et al.* Mean Angular Momenta of Fission Fragments of ^{232}Th // Phys. At. Nucl. 1998. V. 61, No. 9. P. 1562.
21. *Mikhailov I. N., Quentin P., Briacon C. H.* Angular Momentum of Fission Fragments // Phys. At. Nucl. 2001. V. 64, No. 6. P. 1185.
22. *Bezshyyko O. A. et al.* Study of the Mean Angular Momenta of Primary Photofission Fragment of ^{237}Np and ^{238}U // Bull. Univ. of Kiev. 2004. Ser.: Phys. & Math.
23. *Thiep T. D. et al.* Study of the Isomeric Ratio of Fission Product ^{135}Xe Produced in the Photofission of ^{232}Th and ^{233}U Induced by End-Point Bremsstrahlung Energy of 13.5 MeV // Radioanal. Nucl. Chem. 2015. V. 303, No. 1. P. 99.
24. *Lederer C. M., Shirley V. S.* Table of Isotope. 7th Ed. New York; Toronto: John Wiley & Sons Inc., 1978.
25. *Blachot J., Fiche C.* Fission Product Half-Lives and Gammas // At. Data Nucl. Data Tables. 1977. V. 20, No. 3. P. 242.
26. *Thierens H. et al.* Product Yields for Photofission of ^{235}U and ^{238}U with 25-MeV Bremsstrahlung // Phys. Rev. C. 1976. V. 14, No. 3. P. 1058.
27. *Jacob E. et al.* Product Yields for the Photofission of ^{235}U with 12-, 15-, 20-, 30-, and 70-MeV Bremsstrahlungs // Phys. Rev. C. 1980. V. 21, No. 1. P. 237.
28. *Gangrsky Yu. P. et al.* Transportation of the Fission Fragments by the Gas Flow with Aerosol. JINR Preprint P13-2001-66. Dubna, 2001.
29. *Belov A. G., Bondarenko P. G., Teterev Yu. G.* Microtron MT-25. JINR Preprint D15-93-80. Dubna, 1993.
30. *Belov A. G. et al.* Excitation of Isomeric $1h_{11/2}$ States in Nuclear Reactions Induced by Gamma Rays and Neutron in Beta Decay // Phys. At. Nucl. 2001. V. 64, No. 11. P. 1901.
31. *Nesaraja C. D., Sudar S., Qaim S. M.* Cross-Section Ratios for the Formation of ^{69m,g}Zn and ^{71m,g}Zn in Neutron-Induced Reactions near Their Thresholds: Effects of Reaction Channels on the Isomeric Cross-Section Ratios // Phys. Rev. C. 2003. V. 68. 024603.
32. *Qaim S. M., Sudar S., Fessler A.* Influence of Reaction Channel on the Isomeric Cross-Section Ratio // Radiochim. Acta. 2005. V. 93. P. 503.
33. *Thiep T. D. et al.* The Isomeric Ratio of Fragment ^{135}Xe from Photofission of ^{233}U Induced by 23.5-MeV Bremsstrahlung // Radioanal. Nucl. Chem. 2010. V. 285, No. 3. P. 511.
34. *Kopecky J., Gruppelaar H.* Systematics of Neutron-Induced Isomeric Cross-Section Ratio at 14.5 MeV. Netherland Energy Res. Foundation ECN-200. 1987. P. 31.

Received on October 12, 2015.